Science Advances
AAAS

advances.sciencemag.org/cgi/content/full/6/17/eaay1454/DC1

Supplementary Materials for

Vitrification decoupling from α-relaxation in a metallic glass

Xavier Monnier, Daniele Cangialosi*, Beatrice Ruta, Ralf Busch, Isabella Gallino*

*Corresponding author. Email: daniele.cangialosi@ehu.eus (D.C.); i.gallino@mx.uni-saarland.de (I.G.)

Published 24 April 2020, *Sci. Adv.***6**, eaay1454 (2020)
DOI: 10.1126/sciadv.aay1454

This PDF file includes:

Sections S1 to S7
Figs. S1 to S7

SM1. Determination of the thermal fluctuation and the dynamic glass transition temperature

Fig. SM1 shows reversing specific heat data obtained from step response analysis, upon heating, at 10 Hz. In the temperature range investigated, the specific heat of the glass $C_{p,glass}$ and that of the liquid $C_{p,liquid}$, are obtained from the following equations:

$$C_{p,glass}(T) = aT + b \quad \text{(SM1)}$$

$$C_{p,liquid}(T) = 3R + cT + dT^{-2} \quad \text{(SM2)}$$

with a = 0.01 J g-atom^{-1} K^{-2}, b = 22.0 J g-atom^{-1} K^{-1}, c = 13.4 J g-atom^{-1} K^{-2}, d = 2.4 J K g-atom^{-1} and R the ideal gas constant. The coefficients to describe $C_{p,liquid}$ were taken from ref. (17) of the main manuscript, whereas the linear fit of $C_{p,glass}$ is from data of the present work. Such procedure allows to measure the step of the specific heat ΔC_p at the glass transition. The thermal fluctuation δT and the cooperative length scale were estimated by using the following equations (ref. (60) of the main manuscript):

$$\delta T = \Delta T/2.5 \quad \text{(SM3)}$$

valid for a step-protocol in heating, and:

$$\xi = \left(\frac{k_B T_{g,dyn}^2 \Delta\left(\frac{1}{C_p}\right)}{\varrho(\delta T)^2} \right)^{1/3} \quad \text{(SM4)}$$

in which ΔT is the temperature interval where the reversing specific heat curve varies between 16% and 84% of the ΔC_p step, k_B is the Boltzmann constant, δT^2 is the mean-square temperature fluctuation of one average cooperative rearranging region, and ρ is the calculated density of the material (13.127 g cm^{-3}).

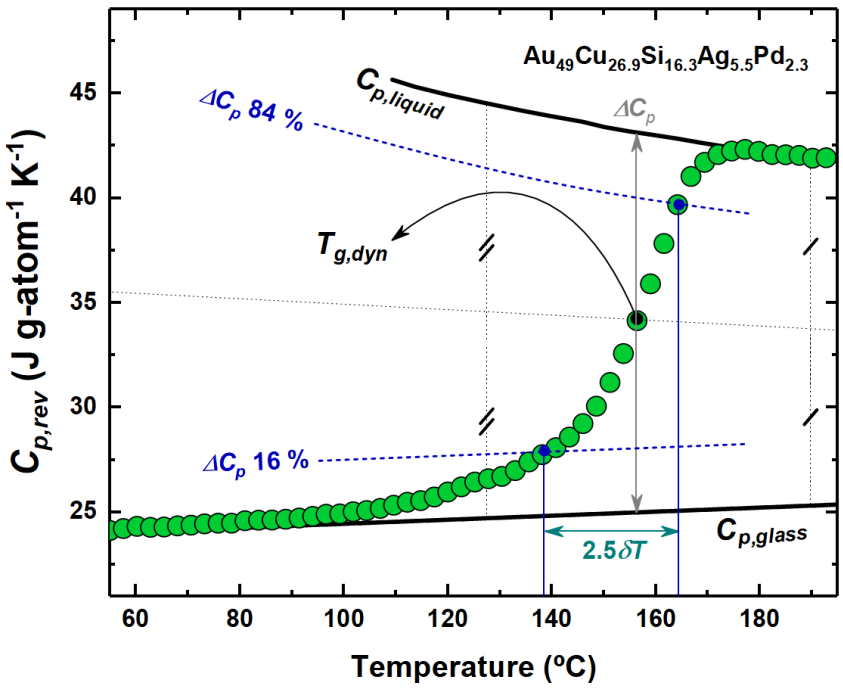

Fig. SM1. Reversing specific heat of the $Au_{49}Cu_{26.9}Si1_{6.3}Ag_{5.5}Pd_{2.3}$ glass-former obtained at 10 Hz by step response analysis.

The dynamic glass transition temperature, $T_{g,dyn}$, is the temperature taken from the midpoint (50%) of the step in $C_{p,rev}$ during the glass transition and $\Delta(1/C_p) = 1/C_{p(glass)} - 1/C_{p(liq)}$, corresponding to the C_p values at 16% and 84% of the step in $C_{p,rev}$. Based on the data reported in Fig. SM1 we obtain a value of ξ = 1.395 ±0.05 nm, and a value for the temperature fluctuation δT of approximately 9 K, which guarantees that the two Kelvin jumps employed in the step response analysis fulfils the linear regime required for rigorous determination of the atomic mobility.

SM2. Determination of T_f

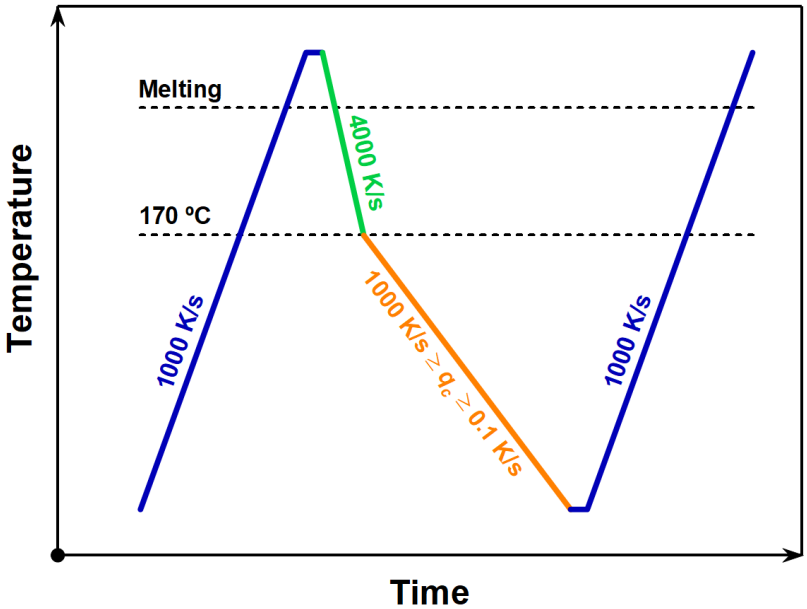

Fig. SM2. Temperature protocol employed to determine T_f.

The thermal protocol employed by the Flash DSC 1 to determine the fictive temperature T_f is shown schematically in Fig. SM2. The sample is first heated up with 1000 K/s to 400 ºC, which is well above the *liquidus* temperature, and after an isothermal step of 0.1 s, the sample is then cooled down to 170 ºC using a cooling rate of 4000 K/s, which was enough to avoid crystallization. Below 170 ºC, the material is further cooled down to -90 ºC, each time with a different rate varying between 0.1 and 1000 K/s, and subsequently heated up to 400 ºC using a heating rate of 1000 K/s, after an isotherm of 0.1 s at -90 °C. During this heating ramp, heat flow rate scans were recorded. The cooling rate dependence of T_f was determined by using the Moynihan area matching method (Ref. (34) of the main manuscript):

$$\int_{T_f}^{T_1 \gg T_g} \left(C_{p,liquid} - C_{p,glass}\right) dT = \int_{T_2 \ll T_g}^{T_1 \gg T_g} \left(C_p - C_{p,glass}\right) dT \qquad \text{(SM5)}$$

in which the $C_{p,glass}$ and the $C_{p,liquid}$ are the specific heat capacity of the glass and the liquid, respectively, as calculated above from eq. SM1 and eq. SM2. The error in terms of T_f is estimated to be ± 2 K, which is smaller than the size of the star symbols in Fig. 3 and in Fig. SM3. Crystallization takes place during cooling when the applied cooling rate is slower than 0.7 K/s, as shown in Fig. 2 of the main text. Therefore, the kinetics of vitrification was characterized only for scans with applied cooling rates between 0.7 and 1000 K/s.

SM3. Determination of the fragility indexes

In Fig. 3 of the main text we show that for the deepest undercooled liquid (T_f = 389 K), which is connected to a very slow cooling protocol (q_c=0.7 K/s), the characteristic time connected to vitrification kinetics is 1.5 orders of magnitude faster than the relaxation time of the α-process. In terms of kinetic fragility the two values given there for the fragility index D^* are, on one hand, characteristic of an extremely highly fragile metallic-glass forming liquid, and, on the other hand, different enough to indicate a decoupling between the α-relaxation and vitrification kinetics. We observe therefore that the decoupling occurs within the fragile regime, well above the fragile-to-strong transition observed for this composition in ref. (47) of the main manuscript.

Fig. SM3 is the same as Fig. 3 of the main text, with the exception that the star symbols, corresponding to the values of T_f, are plotted on the right y-axis as a function of reciprocal of the applied cooling rate, q_c. We would like to show therewith, that the decoupling between the α-relaxation and vitrification kinetics is observed also without converting the cooling rate to a characteristic time scale for vitrification. In this case the decoupling is not observable in terms of timescale but in terms of two different values for the fragility index. In Fig. SM3, the continuous curves represent the VFT fits of the two different sets of data, indicated with two separate legends. The pre-exponential factors are free parameters. Fig. SM3 displays, in agreement with Fig. 3 of the main text, two different values for the fragility index D^*, which are 6.8 and 10.3, respectively.

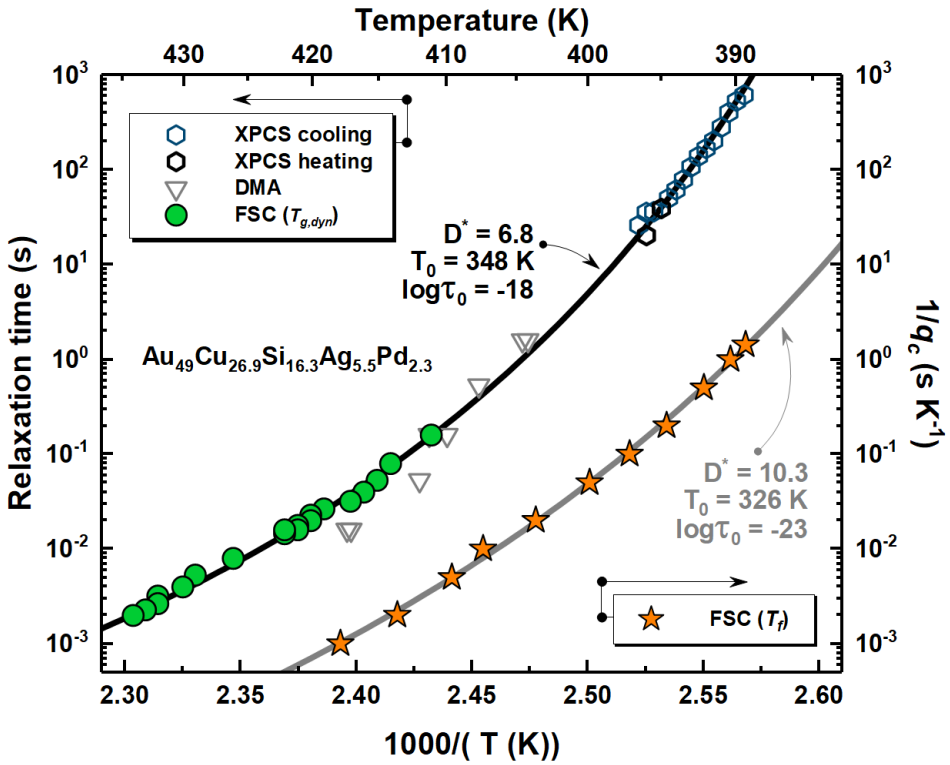

Fig. SM3. Fragility plot for the $Au_{49}Cu_{26.9}Si1_{6.3}Ag_{5.5}Pd_{2.3}$ glass-former in terms of relaxation time associated to the α-relaxation (data sets in top-left legend) in comparison with data representing vitrification kinetics in terms of fictive temperature (data set in bottom-right legend). The values of $1000/T_f$ are plotted as a function of reciprocal of the applied cooling rate, q_c (right y-axis). The lines are fits of the two sets of data to the VFT equation.

SM4. Width of the dynamic vs thermal glass transition

A complementary approach to investigate the relation between α relaxation and vitrification kinetics, proposed by Schawe (Ref. (4) of the main manuscript), is based on the so-called "vitrification function", κ, which is the ratio of the width of transformation from glass to melt, ΔT_{trans} to that of the α-relaxation range, ΔT_α:

$$\kappa = \Delta T_{trans} / \Delta T_\alpha \qquad \text{(SM6)}$$

In this analysis, we consider the whole devitrification range for the determination of ΔT_{trans} (see panel A in Fig. SM4), rather than the glass transition range as identified in Fig. SM5 or SM7, where the Moynihan method was applied. ΔT_α is obtained accounting for the contribution of the α-relaxation process to the step in $C_{p,rev}$ (see for instance Fig. 1 of the main manuscript), since our aim is to verify how this is coupled to vitrification kinetics. To obtain the width of the α-relaxation from XPCS, based on data published in Ref. (43) of the main manuscript, we have calculated the temperature range over which the correlation functions at a time t^*=100 s evolve from their maximum value to a full

decorrelation. We found that the dynamical glass transitions measured with XPCS spans a temperature range of ~17 K at this t*.

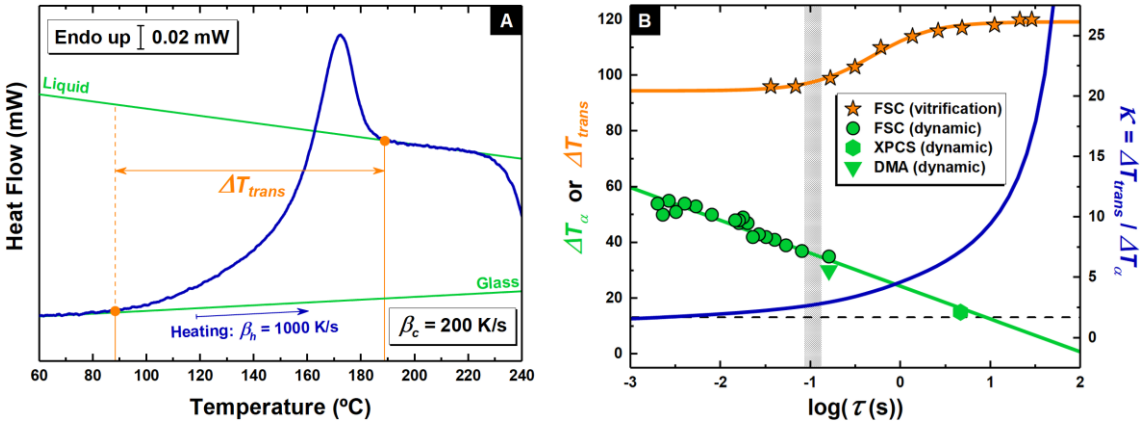

Fig. SM4. Vitrification function versus relaxation time in $Au_{49}Cu_{26.9}Si1_{6.3}Ag_{5.5}Pd_{2.3}$ A) Determination of the range of transformation from glass into melt. B) Relaxation function versus relaxation time (blue line) obtained from the ratio of the widths of the devtrification process (orange stars and line) and the dynamic glass transition (green symbols and line; circles are from FSC of this work; the triangle is from DMA of ref. (36); and the hexagon is from XPCS of ref. (43) of the main manuscript.

As can be observed in Fig. SM4, the vitrification function, κ, exhibits a clear increase with increasing the relaxation time (or equivalently decreasing the cooling rate). Such increase originates from the fact that the width of the dynamic glass transition becomes less pronounced with increasing the relaxation time, as expected from VFT behavior. In contrast, the width of transformation from glass into melt exhibits the opposite behavior based on an increase of ΔT_{trans} with increasing relaxation time. Importantly a significant contribution to this increase comes from the low temperature flank of the devitrification process, that is, the one unrelated to the α-relaxation.

SM5. Glass transition/fictive temperature: heating versus cooling

The method employed in our work to characterize vitrification kinetics relies on the concept of T_f. This is determined employing the Moynihan method (Ref. (34) of the main manuscript), which relies on DSC heating scan. However, some authors (Ref. (61) of the main manuscript) noticed that the glass transition temperature (T_g) obtained on heating may suffer from superheating effects resulting from the employment of the same heating rate as the cooling rate previously employed to vitrify the glass. The

reason for this is that the time spent by the glass on heating is similar to that spent on cooling and, therefore, evolution of the thermodynamic state must be expected during heating as well. In the case of our study, employing the Moynihan method we use heating rates that exceed the previous employed cooling rate. In our work, we set the heating rate at 1000 K/s, whereby the cooling rates are always smaller than or equal to this value. As a result, the T_f obtained by the Moynihan method always coincides with the T_g obtained on cooling. This is shown in Fig. SM5 for one cooling rate, as an example.

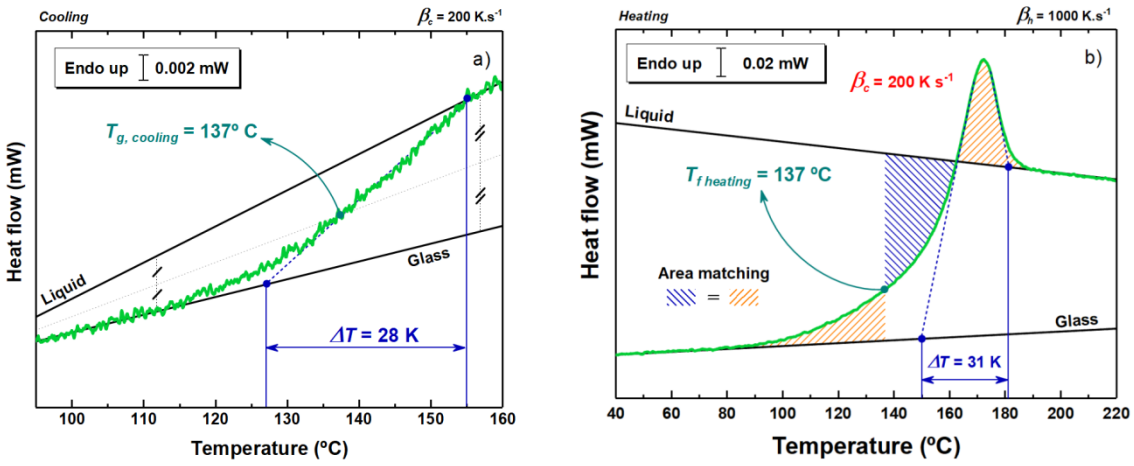

Fig. SM5. Equivalence between glass transition temperature on cooling and fictive temperature (Left panel) Heat flow rate on cooling at the indicated rate and (right panel) on heating at 1000 K/s after cooling at the same rates as the panels on the left.

As can be observed, the T_f obtained in heating and T_g obtained in cooling perfectly coincide. This result is in agreement with previous findings showing the same coincidence between T_f and T_g (see Refs. (62,63) of the main manuscript).

SM6. Heat of crystallization after cooling at different rates

Figure SM6 shows the heat of crystallization, obtained from the integration of heat flow rate scans on heating at 1000 K/s after cooling at different rates. As can be observed, the heat of crystallization is cooling rate independent down to 0.7 K/s, thus indicating at this cooling rate and above samples remains completely amorphous. At lower rates, the heat of crystallization decreases, indicating that on cooling at such rates part of the sample transforms into crystal during such cooling process.

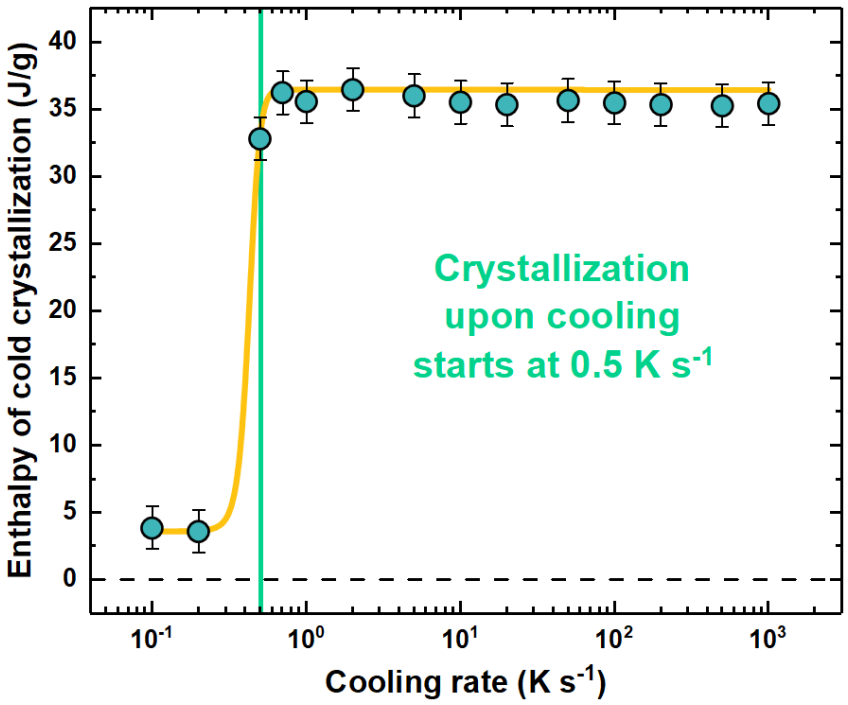

Fig. SM6. Cooling rate dependence of the heat of crystallization.

SM7. Dependence of the glass transition range on the heating rate

The glass transition range, ΔT, is employed to determine the relaxation time associated to vitrification kinetics (see main text). In our work, such range is generally obtained on heating at 1000 K/s. However, it is worth of remark that such range is independent on the employed heating rate. This is demonstrated in Fig. SM7, where heat flow rate scans at different rates after cooling at the same cooling rate (10 K/s) are shown. As can be seen, the glass transition range is independent of the applied heating rate. This result demonstrates the robustness of the relaxation times associated to vitrification kinetics.

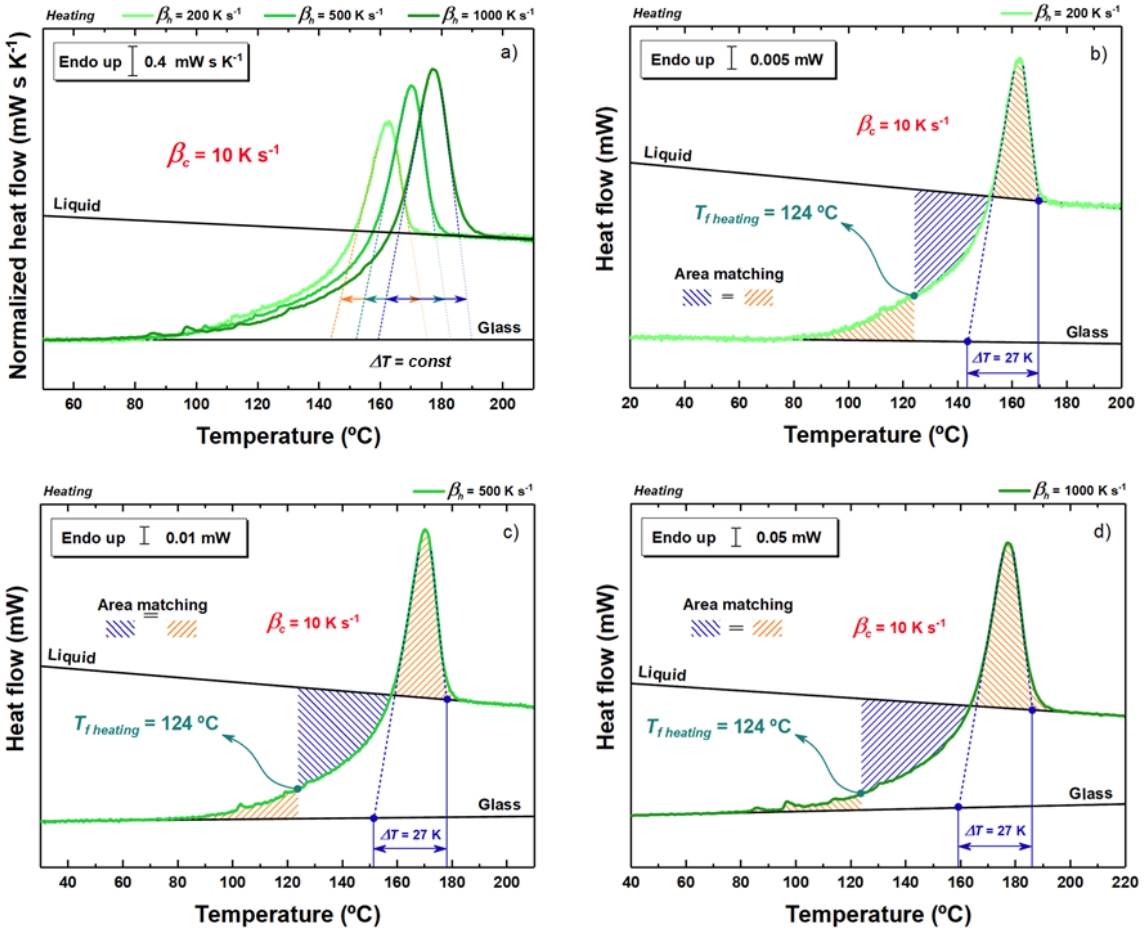

Fig. SM7. Glass transition range determined at different heating rates (Panel a) Heat flow rate scans at different heating rates after cooling at 10 K/s. Panel b-d show in details the determination of the glass transition range at each of the heating rates shown in panel a.